The Effect of Specific β-Nucleation on Morphology and Mechanical Behavior of Isotactic Polypropylene

JIŘí KOTEK,[1] MIROSLAV RAAB,[1] JOSEF BALDRIAN,[1] WOLFGANG GRELLMANN[2]

[1] Institute of Macromolecular Chemistry, Academy of Sciences of the Czech Republic, 162 06 Prague 6, Czech Republic

[2] Institute of Materials Science, Martin Luther University Halle-Wittenberg, D-06099 Halle (S.), Germany

Received 9 February 2001; accepted 13 October 2001

ABSTRACT: The commercial grade of isotactic polypropylene was modified by a specific β-nucleating agent in a broad concentration range. The supermolecular structure of the specimens prepared by injection molding was characterized by X-ray scattering and correlated with mechanical behavior. It was found that at a critical nucleant concentration of 0.03 wt % the content of the β-modification virtually reaches a saturation level. With further addition of the nucleant, the β-phase content increases only slightly. The long period passes through a distinct maximum at the same nucleant concentration. This singularity in structure remarkably correlates with a minimum of the yield stress and maxima of strain at break and fracture toughness. Such general behavior is also reflected in the correlation between the β-phase concentration and fracture toughness profiles along the injection-molded bars. It is suggested that in the critically nucleated material an optimum thickness of the amorphous interlayer with connecting chains between the β-crystallites is established, rendering the material the highest possible ductility and toughness. © 2002 Wiley Periodicals, Inc. J Appl Polym Sci 85: 1174–1184, 2002

Key words: polypropylene; morphology; β-nucleation; mechanical behavior; fracture toughness

INTRODUCTION

Isotactic polypropylene can crystallize in three different modifications, the monoclinic α and the hexagonal β forms, having practical relevance. The hexagonal β-modification can be induced by crystallization in shear fields or in temperature gradients and particularly by specific nucleants. Much attention has been devoted recently to this modification and its effect on important mechanical properties. In particular, it was shown experimentally by several authors[1–12] that the presence of the β-phase within the crystalline portion of the material is beneficial to its macroscopic toughness. Several structural models of this interrelation were offered; however, none of them were generally accepted. Thus, it was suggested[3–5] that the toughening effect is caused by a β-to-α (or smectic) phase transformation at the tip of a growing crack, similar to the mechanism that is effective in zirconia-containing ceramics. Nevertheless, the proposed model also has distinct dissimilarities in respect to engineering ceramics.[8] Alternative approaches try to explain the effect of the β-phase by a specific arrangement of the whole material structure (e.g., by specific

Correspondence to: M. Raab (raab@imc.cas.cz).

Contract grant sponsors: Grant Agency of the Academy of Sciences of the Czech Republic; Grant Agency of the Czech Republic.

Journal of Applied Polymer Science, Vol. 85, 1174–1184 (2002)

spherulites).[9–11] In our previous article,[12] we showed that the profiles of toughness and β-phase concentration along injection-molded specimens of a specific polypropylene grade had strikingly similar trends: both these characteristics markedly decreased with increasing distance from the molding gate. This result illustrates the importance of the shear stresses and cooling rate during solidification of the polypropylene melt on its resulting morphology and the end-use properties. We suggested a model based on the notion that the presence of the β-phase crystallites induces a higher continuity of the amorphous phase and more connecting bridges between individual crystallites than a material containing solely α-crystallites.[12] Better structural continuity is macroscopically reflected as higher drawability and toughness. Clearly, toughness is a matrix-controlled property not only in polymer composites but also in semicrystalline polymers that contain hard crystalline domains embedded in a soft continuous matrix.

On the other hand, our recent results encompassing a broad range of a specific β-nucleant concentrations (0.01–0.13 wt %) indicated that the relation between the β-phase and macroscopic toughness is not straightforward.[13] Although the β-phase content increased monotonically with the amount of the specific β-nucleant, toughness passed through a maximum at a relatively low nucleant concentration (0.03–0.05 wt %). This result shows again that toughness does not directly reflect the structure of the crystalline phase itself. The aim of the present work is to elucidate in more detail the effects of the nucleant concentration and the gradients of structural parameters on the macroscopic mechanical behavior.

EXPERIMENTAL

Sample Preparation

Isotactic polypropylene Mosten 58.412 (Chemopetrol, Litvínov, Czech Republic) was used as a starting material throughout this study. (The same grade but a more recent batch was used as compared with our previous work.[12]) This polymer was modified by a selective β-nucleant NJ-Star NU-100 (Rika International, Manchester, U.K.), based on *N′*,*N′*-dicyclohexylnaphthalene-2,6-dicarboxamide, which was added to polypropylene in the form of a master batch (molecular structure of this compound is shown in Fig. 1).

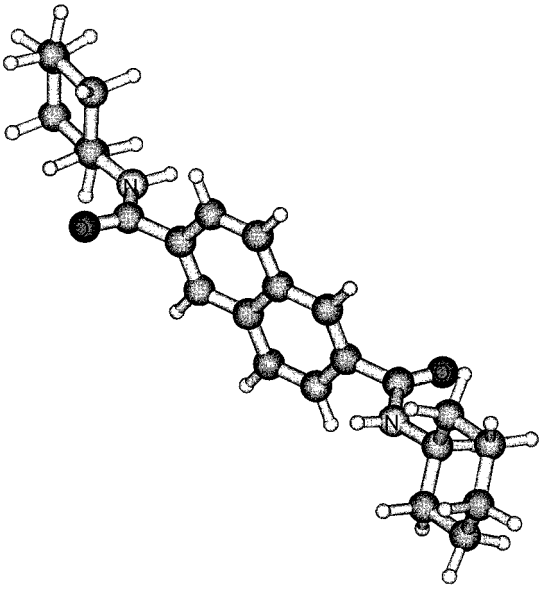

Figure 1 Molecular model of *N′*,*N′*-dicyclohexylnaphthalene-2,6-dicarboxamide, the β-nucleant used in this work.

The concentrations of the nucleant were 0.01, 0.03, 0.05, 0.07, 0.10, and 0.13 wt %.

Test Pieces

Two types of test pieces were prepared by injection molding: standard dumbbell test pieces with gauge length of 50 mm, width of 10 mm, and thickness of 4 mm for tensile measurements and bars for impact testing with dimensions 4 × 10 × 120 mm^3. Single-edge notch specimens for three-point bending impact testing (length, L = 60 mm; width, W = 10 mm; thickness, B = 4 mm) were prepared from the bars. The notches with a depth of 2 mm and a tip radius of 0.2 μm were introduced with a razor blade. The locations of notches along the original molded bar varied, as schematically shown in Figure 2. Eight various locations in the original moldings were selected with the distance D from the molding gate of 30, 40, 50, 60, 65, 70, 80, and 90 mm.

Stress–Strain Measurements

The room temperature tensile testing was performed on an Instron 6025 testing machine according to the ISO 527 standard. The cross-head speed was 50 mm/min except for the Young's modulus determination, which was carried out at a cross-head speed of 1 mm/min. The reported values are averages from 10 measurements.

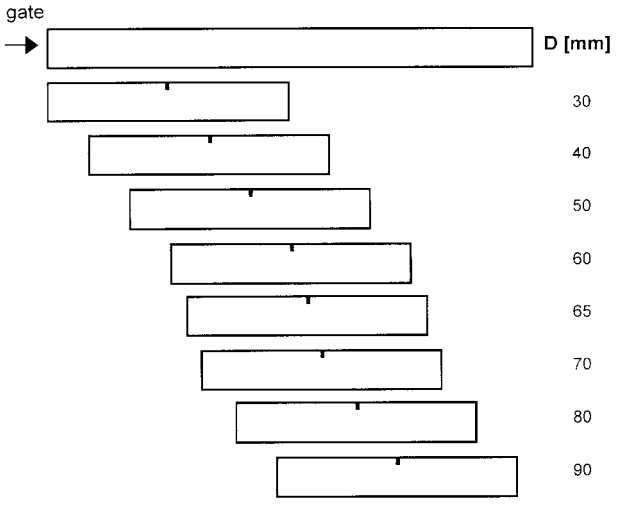

Figure 2 Cutting of individual single-edge notch specimens from injection-molded bars.

Impact Measurements and Calculation of Fracture Toughness

The fracture mechanics testing was carried out on a pendulum Charpy impact tester PSW 4 with 4-J work capacity at the maximum falling height. By use of a Charpy impact device, a single-edge notch specimen is broken by the pendulum hammer impact. The measuring device is able to register load (F)–deflection (f) diagrams. Derived from ISO 179, specimens of thickness $B = 4$ mm, width $W = 10$ mm, and length $L = 80$ mm were used. The notching was carried out at the narrow sides of the specimens up to an initial notch length of 2 mm. The support distance was $s = 40$ mm and the pendulum hammer speed was 1.5 m/s. The values of the J-integral were determined by the following evaluation method proposed by Sumpter and Turner[14]:

$$J_{\mathrm{Id}} = \eta_{\mathrm{el}} = \frac{A_{\mathrm{el}}}{B(W-a)} + \eta_{\mathrm{pl}} \frac{A_{\mathrm{pl}}}{B(W-a)} \frac{W - a_{\mathrm{eff}}}{W-a} \quad (1)$$

where a_{eff} is the crack length at the onset of unstable crack propagation and η_{el}; η_{pl} is the geometry functions for the assessment of elastic (A_{el}) and plastic (A_{pl}) parts of deformation energy up to the maximum load:

$$\eta_{\mathrm{el}} = 0.5 + 5.5(a/W) - 5(a/W)^2 \quad (2)$$

$$\eta_{\mathrm{pl}} = 2 - \frac{(1 - a/W)(0.892 - 4.476a/W)}{1.125 + 0.892(a/W) - 2.238(a/W)^2} \quad (3)$$

For the determination of geometry-independent characteristics of fracture mechanics, the plane–strain state must be ensured [i.e., the geometry values, thickness B, notch depth a, ligament length $(W - a)$, must be higher than certain values]. For that, the following relationships must be fulfilled:

$$B,\ a,\ W - a \geq \varepsilon \frac{J_{\mathrm{Id}}}{\sigma_d} \quad (4)$$

where

$$\varepsilon = 224 J_{\mathrm{Id}}^{-0.94} \quad (5)$$

and σ_d is the dynamic yield stress (see refs.[15,16]). The tests at a given distance D between the notch and the molding gate were repeated 10 times under the same conditions. The toughness of the material with a given nucleant concentration was averaged from the data corresponding to all notch positions.

X-ray Diffraction

Wide-angle X-ray scattering (WAXS) diffraction patterns were obtained by using a powder diffractometer HZG/4A (Freiberger Präzisionsmechanik GmbH, Germany). The total integral intensities I and integral intensities diffracted by crystalline part I_{cr} were used for the determination of crystallinity $X_{\mathrm{c}} = I_{\mathrm{cr}}/I$. The fraction of β-phase in the crystalline phase of polypropylene was calculated by using the following relation[17]

$$K = \frac{I_{300}^{\beta}}{(I_{100}^{\alpha} + I_{040}^{\alpha} + I_{130}^{\alpha} + I_{300}^{\beta})} \quad (6)$$

Crystallite sizes L_{hkl} in the direction perpendicular to (hkl) planes were estimated by using the Scherrer equation $L_{hkl} = \lambda/B \cos\theta$, where λ is the X-ray wavelength, B is the reflection breadth at half-maximum, and 2θ is the scattering angle. For the determination of this structure parameter, the two most intense crystalline reflections (110) and (300) of the α-modification and β-modification, respectively, were selected. Both reflections correspond to the crystal growing planes and, consequently, to the largest lateral dimensions of lamellar crystallites.

Small-angle X-ray scattering (SAXS) patterns were measured on a Kratky camera. After subtracting background, the scattering curves were

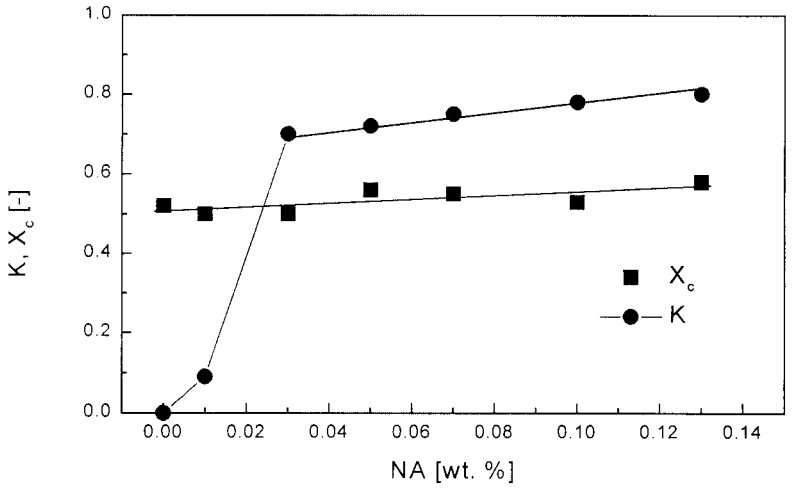

Figure 3 Effect of nucleant concentration NA on the overall crystallinity X_c and fraction K of the β-crystallites within the crystalline phase.

desmeared and Lorentz-corrected. Peak positions on scattering curves were employed to obtain the long-period values LP according to Bragg's law, $LP = 2\pi/q$ [$q = (4\pi/\lambda)\sin\theta$].

SAXS and WAXS patterns of the bar specimens were assessed in the sites corresponding to the notch locations in the single-edge notch specimens (i.e., in the distances 30, 40, 50, 60, 65, 70, 80, and 90 mm from the molding gate). The diffraction patterns were detected in the direction along the bar axis. These measurements produced profiles of the individual structural parameters along the molded bars. Besides, the specimens as a whole were characterized by mean values calculated as averages of the data for the distances 30, 60, and 90 mm from the molding gate.

RESULTS AND DISCUSSION

The Effect of Nucleant Concentration

X-ray Diffraction

The effect of the concentration of the specific nucleant NA on the average values of crystallinity X_c and the β-phase fraction K within the crystalline phase, as assessed by the WAXS analysis, is presented in Figure 3. Two important conclusions can be derived from the presented data. First, it can be seen that the overall crystallinity X_c monotonically but very slowly grows from 50 to 58% with the nucleant content increasing from 0 to 0.13 wt %. Second, it is demonstrated that a certain critical concentration of the nucleation agent (about 0.03 wt %) is necessary to obtain a marked effect on the β-phase content. The sample prepared without any nucleant contained solely α-crystallites and polypropylene modified by 0.01 wt % of the nucleant contained only 9 wt % of the crystalline β-phase. When the nucleant concentration reached the critical value of 0.03 wt %, the fraction K of the β-crystallites within the crystalline phase steeply increased up to 70%. With further increasing the nucleant concentration between 0.03 and 0.13, the fraction K of the β-modification slowly but monotonically increased (from 70 to 80 wt %), following a similar trend to the overall crystallinity. These results seem to indicate that a sufficient number of specific nuclei is necessary for polypropylene to predominantly crystallize into the β-phase. Additional nuclei then have only a minor effect.

Lateral sizes of crystallites (measured perpendicularly to the chain axes) for the two crystalline modifications $L_{110}(\alpha)$ and $L_{300}(\beta)$ obtained by WAXS are presented in Figure 4 as a function of the nucleant concentration NA. Again, two observations can be derived from this figure. First, the dimensions of β-crystallites are approximately three times larger than the corresponding dimensions of α-crystallites. This result could be ascribed to a higher growth rate of the β-crystallites. Second, the sizes of both α- and β-crystallites show a small but significant decrease for the lowest nucleant concentration and by increasing further the nucleant concentration remain virtually constant.

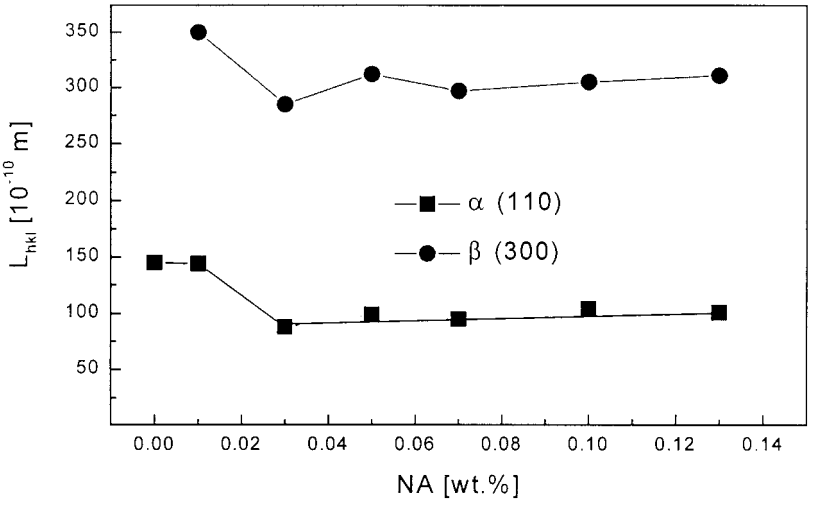

Figure 4 Effect of nucleant concentration NA on the lateral sizes L_{hkl} of the α-crystallites and β-crystallites.

The particular structure corresponding to the critical nucleant concentration range is markedly expressed in the data of the long period LP. The dependence of LP on the nucleant concentration NA, as obtained by SAXS, is shown in Figure 5. A pronounced broad maximum appears for the NA range of 0.03–0.05 wt %. By further increasing the NA, the LP decreases again. In the case of SAXS, no difference between α- and β-crystalline structure could be found within the experimental precision. The geometrical arrangements of α-crystallites in neat polypropylene and β-crystallites in critically β-nucleated sample are schematically shown in Figure 6.

Tensile Mechanical Behavior

The following mechanical characteristics were derived from the stress–strain diagrams: yield stress, yield strain, tensile stress at break, and tensile strain at break. Before discussing them individually, it is interesting to note that the critical nucleant concentration (0.03 wt %) is imprinted in a particular way in all these characteristics. Figure 7 shows the variation of yield stress and yield strain versus nucleant concentration NA. It can be seen that the yield strain is not significantly modified up to the critical nucleant concentration of 0.03 wt %, when it reaches the

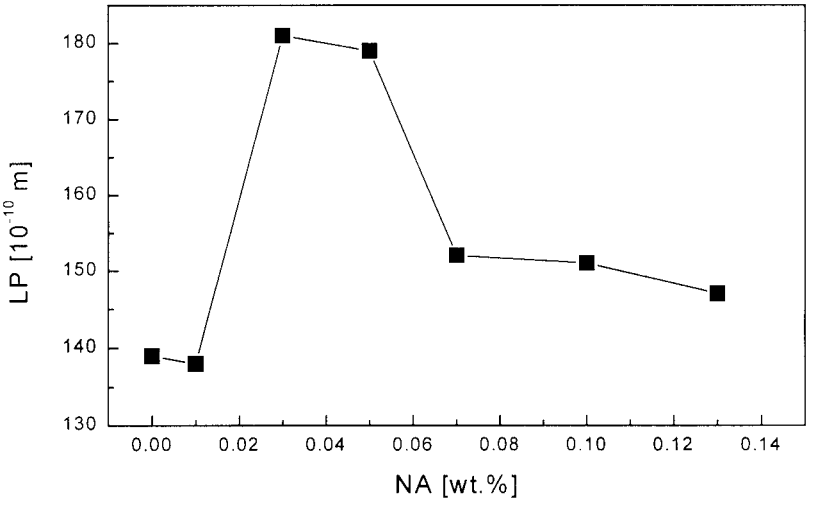

Figure 5 Effect of nucleant concentration NA on the long period LP.

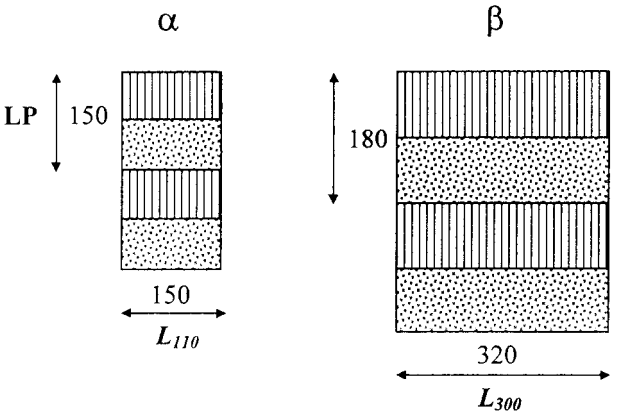

Figure 6 Schematic representation of two-phase structure of neat isotactic polypropylene containing solely α-crystallites and critically β-nucleated polypropylene. Characteristic values of long-period LP and lamellar size L_{khl} are indicated (in 10^{-10} m).

value of 6.4%. Beyond this point, yield strain slightly but monotonically decreases down to 4.6% for the nucleant concentration of 0.13 wt %. On the other hand, the yield stress drops from 37.6 MPa for the nonmodified polymer to a minimum value of 29.9 MPa for the critical concentration and then increases again up to 34.9 MPa. This shallow but significant minimum of the yield stress indicates an enhanced compliance of the material just at the critical nucleant concentration. (We observed that the value of Young's modulus E showed a similar course with a minimum at the critical nucleant concentration.)

The enhanced compliance and ductility of the critically nucleated material is even more pronounced for the tensile strain at break. The data are plotted in Figure 8 together with the stress at break as a function of the nucleant concentration. It is shown that tensile strain at break passes through a distinct maximum. It increases dramatically from 72.6% for the starting polymer to 492% for the critically nucleated material and then decreases steeply again down to 72.5% for the highest nucleant concentration. Obviously, the highest value of the tensile strain at break reflects an extensive cold drawing by neck propagation. The resulting high molecular orientation, in turn, imparts high tensile strength to the drawn material. Indeed, the maximum tensile stress at break virtually coincides with the maximum tensile strain at break. Tensile stress at break increases from 16.6 MPa for the starting polymer to 31.1 MPa for the critically nucleated material and then decreases to 23.6 MPa for the highest nucleant concentration. Consequently, the plot of tensile stress at break versus nucleant concentration is virtually a mirror image of the corresponding plot of the yield stress. These two plots intersect just at the critical nucleant concentration, and only in this case of critically nucleated polymer, the stress at break surpasses the value of the yield stress. (Clearly, the values of tensile stress at break and tensile strain at break exhibit substantially higher scatter than the corresponding values at the yield point.)

Toughness Behavior

The enhancement of ductility and orientational drawing of polypropylene by the presence of the crystalline β-phase was also reflected in an increased toughness under impact loading conditions. Figure 9 shows the effect of the nucleant concentration NA on the toughness characterized by the critical J_{Id} value of the J-integral. The J_{Id} values increase markedly from 2.5 N/mm for the nonnucleated polypropylene to 10.5 N/mm for the polypropylene with the critical nucleant concentration of 0.3 wt %. The analysis of the corresponding F–f diagrams showed that this rise is determined by an increase of both $F_{\max}$ and $f_{\max}$ as functions of increasing nucleant concentration. Thus, the toughness increase is energy-determined and the J_{Id} value is a geometry-independent polymer-specific toughness parameter. Higher local ductility of the critically nucleated material as compared to nonmodified polypropylene is documented by scanning electron micrographs of the corresponding fracture surfaces (Fig. 10). It should be noted that the extreme values of important mechanical characteristics (yield stress, yield

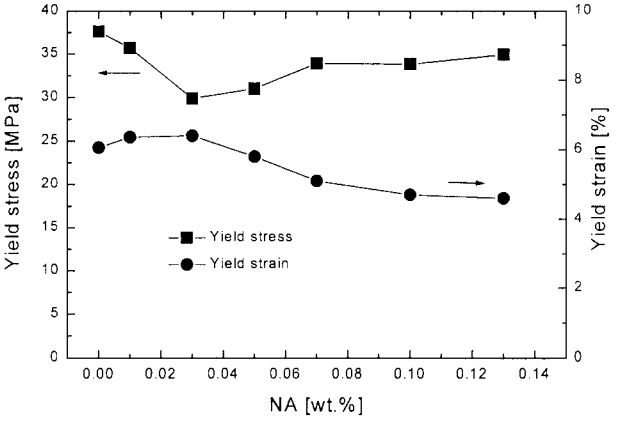

Figure 7 Effect of nucleant concentration NA on the yield stress and the yield strain.

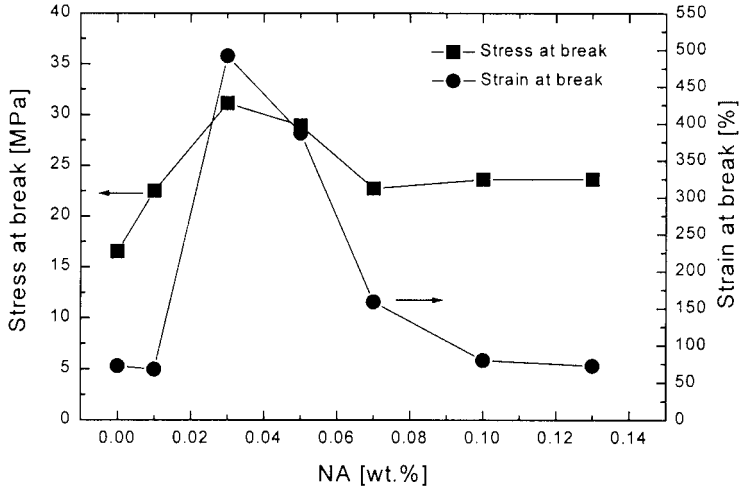

Figure 8 Effect of nucleant concentration NA on the tensile stress at break and the tensile strain at break.

strain, tensile strain at break, tensile stress at break toughness, and Young's modulus) clearly correlate with the distinct maximum of the long period.

Structure and Property Gradients

The gradients of morphological parameters and toughness characteristics along the injection-molded bars were assessed with neat material and samples containing 0.03 and 0.05 wt % of the β-nucleating agent.

Morphology Profiles

WAXS and SAXS study of structure parameters profiles along test specimens has shown that crystallinity, lateral dimension of α-crystallites and β-crystallites, and long period values do not change significantly with increasing distance D from the molding gate and retain the average values reported above. Figure 11 shows that the content of the β-phase grows with increasing distance D, and fraction K is higher for the higher nucleant content. No β-crystallites were detected in the case of neat material along the whole length of injection-molded bars. These results demonstrate that the fact that the structure of the test bars is not homogeneous reflects the conditions of sample preparation. Obviously, the gradients of temperature and shear stress in the mold cavity during its filling induce corresponding gradients of crystalline structure, molecular

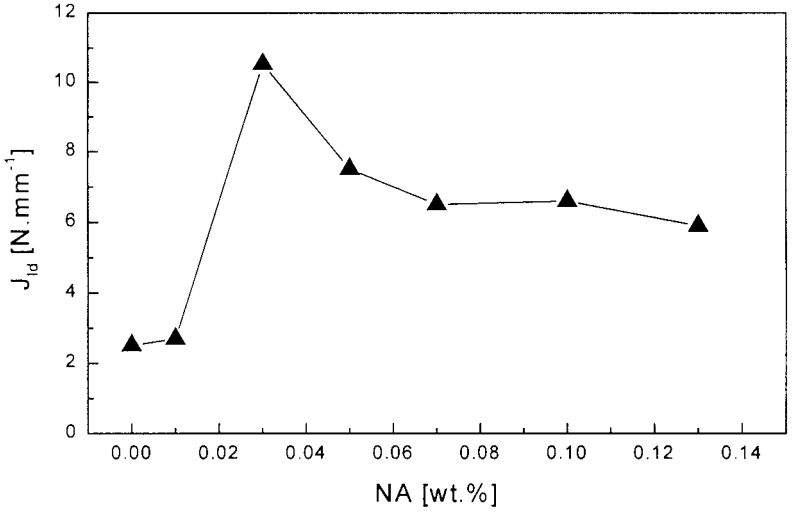

Figure 9 Effect of nucleant concentration NA on the toughness J_{Id}.

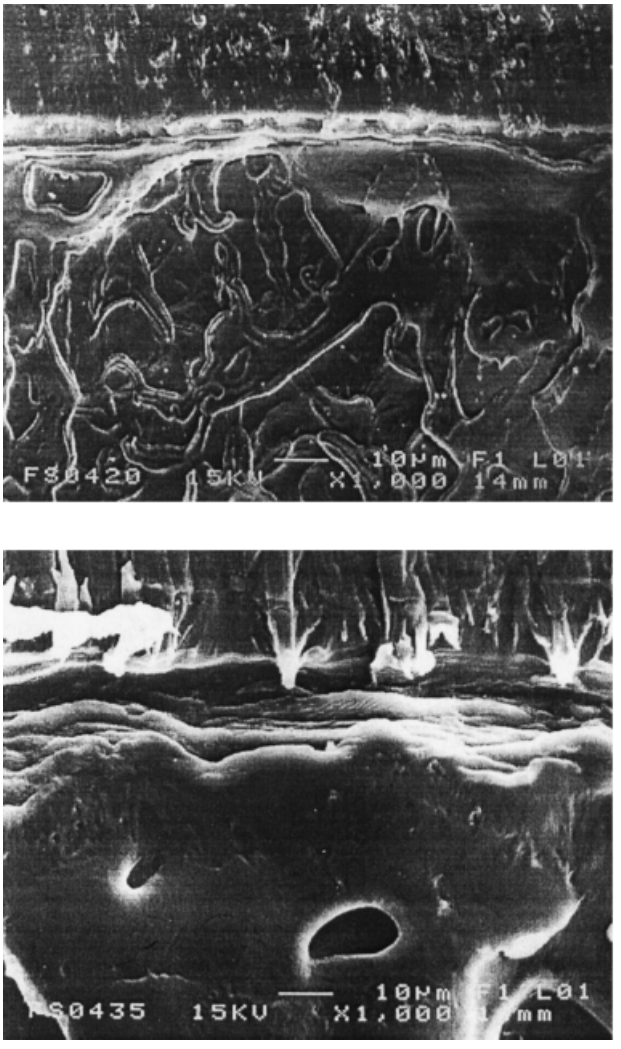

Figure 10 SEM micrographs showing single-edge notch specimens of (a) unmodified polypropylene and (b) polypropylene nucleated with 0.03 wt % of the β-nucleant, broken at room temperature. The introduced notches can be seen in the top of the pictures. Note the distinctly higher local plasticity in the nucleated material.

orientation, skin-core effect, and, consequently, macroscopic mechanical properties.

Toughness Profiles

In Figures 12 and 13 the profiles of toughness characterized by J_{Id} values are presented for room temperature and for −30°C. The data for room temperature show markedly higher toughness for the lower β-phase content and, in contrast to neat polypropylene, the values vary distinctly along the injection-molded bar. For the specimen portion adjacent to the molding gate, an increase in J_{Id} values with increasing distance is observed. The J_{Id} value passes through a maximum and then monotonically decreases again. Simultaneously with the variation of these values, the nature of the load-deflection records of the impact tests also varies. Typical examples of these characteristic records for different distances from the molding gate are presented in Figure 12. It can be seen that the material close to the molding gate shows a stable crack growth. With increasing distance, a clear tendency to unstable crack growth is manifested. Consequently, the J_{Id} data for the lower distances do not reflect a real material toughness J_{Id}, as they do not include the energy dissipated by stable crack propagation. Therefore, these values are not valid

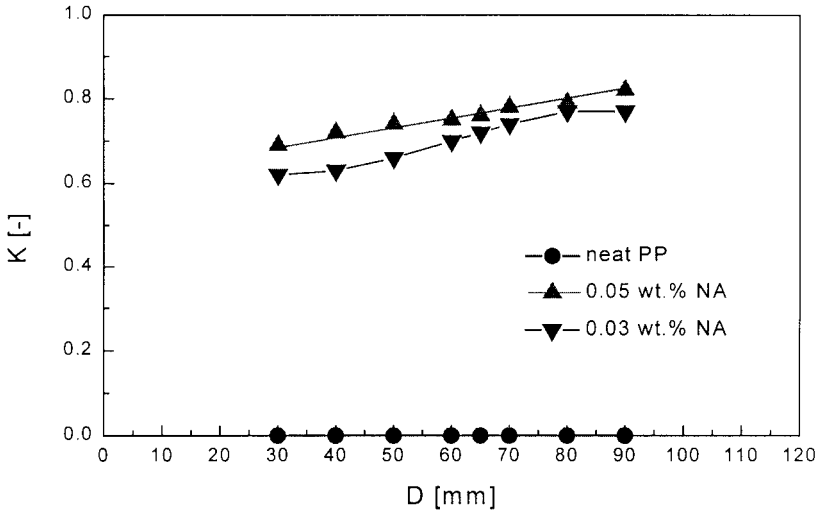

Figure 11 Fraction K of β-crystallites versus distance D from the molding gate.

from the viewpoint of the fracture mechanics concept. (Real toughness characteristics should be increased by that contribution.)

In Figure 13, the toughness profiles for −30°C are presented. An overall decrease in toughness as compared to room temperature values manifests itself for all three materials, but particularly for the nucleated samples. Nevertheless, the increase caused by the presence of the β-phase is maintained along the length of injection-molded bars and is higher again for the sample containing the critical nucleant concentration (0.03 wt %). It should be noted that at −30°C, all specimens broke in an unstable manner.

A comparison of Figures 11–13 shows that no straightforward correlation between the β-phase

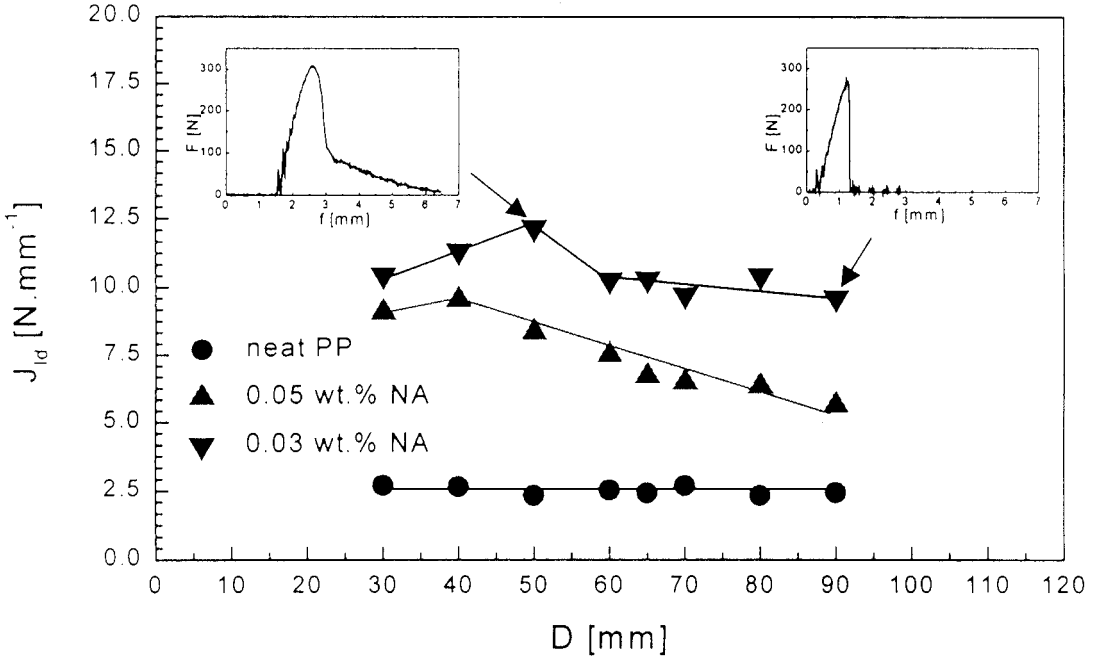

Figure 12 Fracture mechanics J_{Id} values at room temperature versus distance D from the molding gate. Inserts show typical load (F)–deflection (f) diagrams for the indicated distances D.

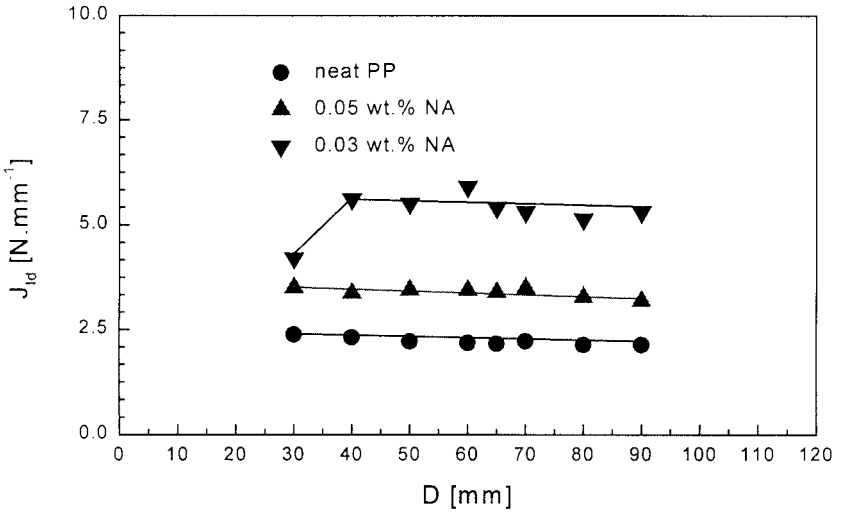

Figure 13 J_{Id} at −30°C versus distance D from the molding gate.

content and macroscopic toughness behavior can be drawn. Not even morphological parameters can explain the observed toughness profiles. Therefore, it is likely that the nonmonotonic course of J_{Id} values as a function of the notch-gate distance of nucleated samples reflects the molecular orientation and skin-core effect created during the filling of the mold cavity.

Structural Model

Three experimental results important for the formulation of a structure model should be stressed. First, none of the mechanical characteristics followed in this study depend monotonically on the concentration of the nucleant or on the proportion of the β-phase, but all parameters show a singularity at a critical nucleant concentration (0.03 wt %). A local minimum of modulus, a minimum of the yield stress, a maximum of crack resistance against unstable crack propagation, and particularly a maximum of tensile strain at break occur at this point. Second, the size of crystallites as assessed by WAXS shows a minimum at the same nucleant content. Third, the long period, as detected by the SAXS, passes through a broad but distinct maximum in the same concentration range. This means that the aspect ratio of the β-crystallites also has a minimum and the thickness of the amorphous layer between crystallites reaches a maximum value in this region.

Therefore, the results of the present study demonstrate the role of the amorphous matrix between the β-crystallites. In particular, the striking correlation between the maxima of long period, tensile strain at break, and crack resistance to unstable crack propagation at the same critical nucleant concentration of 0.03 wt % shows the important role played by the amorphous interlayer between crystallites in deformation and fracture processes. Indeed, higher thickness of the amorphous layer with many connecting chains facilitates plastic deformation and, consequently, molecular orientation. Such mechanism can be effective in the bulk of the material but obviously also at the notch tip, as demonstrated by scanning electron micrographs [Fig. 10(a,b)]. Further increase in the nucleant content beyond the critical concentration decreases the optimum thickness of the amorphous interlayer again. At the same time, the results of this comprehensive study suggest that we have to revise our explanation model published earlier,[12] as it does not show the lamellar periodicity.

CONCLUSIONS

(1) For a specific β-nucleation agent, a critical concentration (of about 0.03 wt %) was found, necessary to obtain a significant fraction of the crystalline β-phase. With further increase in the nucleant concentration, the fraction of the β-phase increases only slightly.
(2) The morphology of the nucleated samples shows specific features at a critical β-nucleant concentration: a minimum of lateral dimensions of the crystallites and a distinct maximum of the long period.

(3) All the investigated mechanical properties display an extreme value at the critical β-nucleant concentration: yield stress and Young's modulus pass through minima, whereas yield strain, tensile strain at break, tensile stress at break, and crack resistance to unstable crack propagation exhibit maxima.
(4) Morphological parameters do not vary significantly along the injection-molded bars with the exception of the β-phase content, which increases monotonically with increasing distance from the molding gate. On the other hand, crack resistance shows a maximum in the vicinity of the molding gate and then slightly decreases with increasing distance. This behavior reflects the orientation created during injection molding.
(5) A structural model is presented on the basis of the role of the amorphous phase. It is suggested that the thickest amorphous interlayers formed in the critically nucleated material render the optimum material ductility and crack resistance.

The authors are grateful to the Grant Agency of the Academy of Sciences of the Czech Republic and to the Grant Agency of the Czech Republic for support (Projects A4050904, 106/98/0717, 106/99/P011). We thank Dipl.-Phys. W. Hesse, Institute of Materials Science, Martin Luther University Halle-Wittenberg, Germany for carrying out the experiments for toughness characterization and Dr. Ladislav Pospíšil, Polymer Institute Brno, Czech Republic for donation of nucleant sample and valuable discussions.

REFERENCES

1. Varga, J. in Crystallization, melting and supermolecular structure of isotactic polypropylene; Karger-Kocsis, J., Ed.; Polypropylene: Structure, Blends and Composites; Chapman & Hall: London, 1995; Vol. 1, Chapter 3, pp 56–115.
2. Varga, J.; Ehrenstein, G. W. in Beta-modification of isotactic polypropylene; Karger-Kocsis, J., Ed.; Polypropylene, An A–Z Reference; Kluwer Academic: Dordrecht, 1999; pp 51–59.
3. Karger-Kocsis, J. J Polym Eng Sci 1996, 36, 203.
4. Karger-Kocsis, J.; Varga, J.; Ehrenstein, G. W. J Appl Polym Sci 1997, 64, 2057.
5. Karger-Kocsis, J.; Varga, J. J Appl Polym Sci 1996, 62, 291.
6. Varga, J., Breining, A., Ehrenstein, G. W., Bodor G. Int Polym Process 1999, 14, 358.
7. Fujiyama, M. Int Polym Process 1995, 10, 172.
8. Karger-Kocsis, J. in Fracture and fatigue behaviour of semicrystalline polymers as a function of microstructural and molecular parameters; Cunha, A. M., Fakirov, S., Eds.; Structure Development During Polymer Processing; Kluwer: Dordrecht, 2000; p 163.
9. Tjong, S. C.; Li, R. K. Y.; Cheung, T. Polym Eng Sci 1997, 37, 166.
10. Tjong, S. C.; Cheung, T.; Li, R. K. Y. Polym Eng Sci 1996, 36, 100.
11. Li, J. X.; Cheung, W. L. Polymer 1998, 39, 6935.
12. Raab, M.; Kotek, J.; Baldrian, J.; Grellmann, W. J Appl Polym Sci 1998, 69, 2255.
13. Kotek, J.; Baldrian, J.; Raab, M. The interrelation between supermolecular structure and tensile mechanical properties of isotactic polypropylene, in IUPAC MACRO 2000, Book of Abstracts; Polish Chemical Society: Warsaw, 2000; Vol. 1, p 349.
14. Sumpter, J. D.; Turner, C. E. Int J Fracture 1973, 9, 320.
15. Grellmann, W.; Che, M. J Appl Polym Sci 1997, 66, 1237.
16. Grellmann, W.; Seidler, S. Eds. Deformation and Fracture Behaviour of Polymers; Springer: Berlin, Heidelberg, 2001.
17. Turner Jones, A.; Aizlewood, J. M.; Beckett, D. R. Makromol Chem 1959, 75, 134.